**Atmospheric
Chemistry
and Physics
Discussions**

Kinetic double-layer model of aerosol surface chemistry and gas-particle interactions (K2-SURF): degradation of polycyclic aromatic hydrocarbons exposed to O_3, NO_2, H_2O, OH and NO_3

M. Shiraiwa, R. M. Garland, and U. Pöschl

Max Planck Institute for Chemistry, Department of Biogeochemistry, J. J. Becherweg 27/29, 55128 Mainz, Germany

ACPD

9, 18021–18063, 2009

Kinetic double layer model (K2-SURF)

M. Shiraiwa et al.

Title Page

Abstract	Introduction
Conclusions	References
Tables	Figures

◄ | ►I

◄ | ►

Back | Close

Full Screen / Esc

Printer-friendly Version

Interactive Discussion

Abstract

We present a kinetic double-layer surface model (K2-SURF) that describes the degradation of polycyclic aromatic hydrocarbons (PAHs) on aerosol particles exposed to ozone, nitrogen dioxide, water vapor, hydroxyl and nitrate radicals. The model is based on multiple experimental studies of PAH degradation and on the PRA framework (Pöschl et al., 2007) for aerosol and cloud surface chemistry and gas-particle interactions.

For a wide range of substrates, including solid and liquid organic and inorganic substances (soot, silica, sodium chloride, octanol/decanol, organic acids, etc.), the concentration- and time-dependence of the heterogeneous reaction between PAHs and O_3 can be efficiently described with a Langmuir-Hinshelwood-type mechanism. Depending on the substrate material, the Langmuir adsorption constants for O_3 vary over three orders of magnitude ($K_{ads,O_3} \approx 10^{-15} - 10^{-13}$ cm^3), and the second-order rate coefficients for the surface layer reaction of O_3 with different PAH vary over two orders of magnitude ($k_{SLR,PAH,O_3} \approx 10^{-18} - 10^{-17}$ cm^2 s^{-1}). The available data indicate that the Langmuir adsorption constants for NO_2 are similar to those of O_3, while those of H_2O are several orders of magnitude smaller ($K_{ads,H_2O} \approx 10^{-18} - 10^{-17}$ cm^3). The desorption lifetimes and adsorption enthalpies inferred from the Langmuir adsorption constants suggest chemisorption of NO_2 and O_3 – possibly in the form of O atoms – and physisorption of H_2O.

The K2-SURF model enables the calculation of ozone uptake coefficients, γ_{O_3}, and of PAH concentrations in the quasi-static particle surface layer. Competitive adsorption and chemical transformation of the surface (aging) lead to a strong non-linear dependence of γ_{O_3} on time and gas phase composition, with different characteristics under dilute atmospheric and concentrated laboratory conditions. Under typical ambient conditions, γ_{O3} of PAH-coated aerosol particles are expected to be in the range of $10^{-6} - 10^{-5}$.

At ambient temperatures, NO_2 alone does not efficiently degrade PAHs, but it was

found to accelerate the degradation of PAHs exposed to O_3. The accelerating effect can be attributed to highly reactive NO_3 radicals formed in the gas phase or on the surface. Estimated second-order rate coefficients for O_3-NO_2 and PAH-NO_3 surface layer reactions are in the range of 10^{-17}–$10^{-16}\,cm^2\,s^{-1}$ and 10^{-15}–$10^{-12}\,cm^2\,s^{-1}$, re-
5 spectively.

The chemical half-life of PAH is expected to range from a few minutes on the surface of soot to multiple hours on organic and inorganic solid particles and days on liquid particles. On soot, the degradation of particle-bound PAHs in the atmosphere appears to be dominated by a surface layer reaction with adsorbed ozone. On other substrates,
10 it is likely dominated by gas-surface reactions with OH or NO_3 radicals (Eley-Rideal-type mechanism). To our knowledge, K2-SURF is the first atmospheric process model describing multiple types of parallel and sequential surface reactions between multiple gaseous and particle-bound chemical species. It illustrates how the general equations of the PRA framework can be simplified and adapted for specific reaction systems,
15 and we suggest that it may serve as a basis for the development of a general master mechanism of aerosol and cloud surface chemistry.

1   Introduction

Aerosols are ubiquitous in the atmosphere and have strong effects on climate and public health. Depending on chemical composition and surface properties, aerosol parti-
20 cles can act as condensation nuclei for cloud droplets and ice crystals, and they can influence trace gas concentrations through heterogeneous chemical reactions (Seinfeld and Pandis, 1998; Pöschl, 2005; Fuzzi et al., 2006; Andreae and Rosenfeld, 2008; Hallquist et al., 2009). Polycyclic aromatic hydrocarbons (PAHs) are one of the most prominent groups of toxic air pollutants. They originate from biomass burning and fos-
25 sil fuel combustion, and they reside to a large extent in fine air particulate matter that can penetrate deep into human lungs (Finlayson-Pitts and Pitts, 2000; Pöschl, 2002; Schauer et al., 2003). Chemical degradation and transformation (oxidation or nitration)

can change the surface properties of aerosol particles and the toxicity of PAH (Pitts, 1983; Atkinson and Arey, 1994; Pöschl, 2002; Schauer et al., 2004; Pöschl et al., 2007).

Moreover, PAH as well as its oxygenated or nitrated derivatives are well defined model substances for the molecular structure of soot, which is the black solid product of incomplete combustion or pyrolysis of organic matter (Homann, 1998; Messerer et al., 2005; Pöschl, 2005; Sadezky et al., 2005). Soot contributes to regional and global climate change because of its role in direct, indirect and semi-direct radiative forcing (Hansen et al., 1997; Ackerman et al., 2000; Jacobson, 2000). Upon emission from combustion sources, fresh soot is initially hydrophobic and mostly externally mixed with non-refractory compounds (Shiraiwa et al., 2007; Schwarz et al., 2008). However, condensation of semi-volatile compounds and chemical processing by ozone and other oxidants can make soot particles hydrophilic (Mikhailov et al., 2006) and influence their ability to act as cloud condensation nuclei (Kuwata et al., 2007). Furthermore, chemical reactions with atmospheric photo-oxidants can lead to substantial degradation, short-term and seasonal variations, and measurement artefacts in the determination of PAHs (Schauer et al., 2003; Marchand et al., 2004; Schauer et al., 2004; Liu et al., 2006; Lee and Kim, 2007; Lammel et al., 2009).

As detailed below (Sect. 3), several laboratory studies have investigated the heterogeneous reaction of PAHs on various substrates with ozone, nitrogen dioxide, water vapor, hydroxyl and nitrate radicals. So far, however, the experimental results had not yet been compiled in a form that enables efficient modelling of PAH degradation in different types of reaction systems and direct comparison of relevant physicochemical parameters (accommodation, uptake, and reaction rate coefficients; adsorption constants; etc.).

Recently, Springmann et al. (2009) have demonstrated the applicability and usefulness of the PRA framework (Ammann and Pöschl, 2007; Pöschl et al., 2007) for atmospheric modeling of the degradation of benzo[a]pyrene on soot by ozone and nitrogen dioxide. In this study we show that the PRA model approach can be efficiently extended

to other PAHs and photo-oxidants. Within the European integrated project on aerosol, cloud, climate and air quality interactions (EUCAARI) (Kulmala et al., 2009), we have reviewed and synthesized available literature data to develop a reaction mechanism describing the degradation of PAHs exposed to O_3, NO_2, H_2O, OH and NO_3 radicals in a kinetic double-layer surface model (K2-SURF). PAH degradation and related ozone uptake are simulated over a wide range of conditions, and the atmospheric implications are discussed.

2   Model description

The K2-SURF model is based on the PRA framework for aerosol and cloud surface chemistry and gas-particle interactions (Pöschl et al., 2007; Ammann and Pöschl, 2007). This framework describes the gas-particle interface by several model compartments and molecular layers in which volatile, semi-volatile and non-volatile species can undergo mass transport and chemical reactions: gas phase, near-surface gas phase, sorption layer, quasi-static surface layer, and (near-surface) bulk of the particle.

As illustrated in Fig. 1, the K2-SURF model does not consider semi-volatile species and processes in the particle bulk, which is just regarded as a substrate that may influence the properties of the quasi-static surface layer.

In describing the degradation of particle-bound polycyclic aromatic hydrocarbons (PAHs) exposed to O_3, H_2O, NO_2, OH, and NO_3, the focus was on the gas phase diffusion, gas-surface mass transport, surface layer reactions, and gas-surface reactions, which are discussed in following sections. We assumed that the effects of surface-bulk mass transport and chemical reactions in the bulk are negligible compared to gas-surface mass transport and chemical reactions at the surface.

2.1 Gas phase diffusion and gas-surface mass transport

Based on kinetic theory, the gas kinetic flux of X_i colliding with the surface J_{coll,X_i} can be expressed as

$$J_{\text{coll},X_i} = [X_i]_{\text{gs}} \omega_{X_i}/4 \qquad (1)$$

where $[X_i]_{\text{gs}}$ is near-surface gas phase concentration of X_i and ω_{X_i} is mean thermal velocity given by $\omega_{X_i}=(8RT/(\pi M_{X_i}))^{1/2}$, where M_{X_i} is the molar mass of X_i, R is the gas constant, and T is the absolute temperature. Here we assume that the gas phase concentrations of O_3, H_2O, and NO_2 are homogeneous throughout gas phase and near-surface gas phase ($[X_i]_{\text{gs}}=[X_i]_{\text{g}}$). This assumption is well justified when uptake coefficients are below 10^{-3} (Ammann and Pöschl, 2007).

On the other hand, uptake of OH and NO_3 by PAH is reported to be high (>0.1) (Bertram et al., 2001; Gross and Bertram, 2008), therefore, the significant net uptake of OH and NO_3 will lead to local depletion of concentration at near-surface gas phase ($[X_i]_{\text{gs}}<[X_i]_{\text{g}}$) and gas phase diffusion will influence further uptake. In this case near-surface gas phase concentration should be corrected using a gas phase diffusion correction factor C_{g,X_i}.

$$[X_i]_{\text{gs}}=C_{\text{g},X_i}[X_i]_{\text{g}} \qquad (2)$$

C_{g,X_i} can be described as follows based on PRA framework (Pöschl et al., 2007).

$$C_{\text{g},X_i} = \cfrac{1}{1 + \gamma_{X_i} \cfrac{0.75+0.28 Kn_{X_i}}{Kn_{X_i}(1+Kn_{X_i})}} \qquad (3)$$

Kn_{X_i} is Knudsen number which can be approximated by gas phase diffusion coefficient D_{g,X_i} and particle diameter d_{p}.

$$Kn_{X_i} = \frac{6D_{\text{g},X_i}}{\omega_{X_i} d_{\text{p}}} \qquad (4)$$

Printer-friendly Version

Interactive Discussion

Using the reported value of $D_{g,OH}=163\,\mathrm{Torr\,cm^2\,s^{-1}}$ (Ivanov et al., 2007), $\gamma_{OH}=0.32$ (Bertram et al., 2001), $D_{g,NO_3}=80\,\mathrm{Torr\,cm^2\,s^{-1}}$ (Rudich et al., 1996) and $\gamma_{NO_3}=0.13$ (Gross and Bertram, 2008), $C_{g,OH}$ and C_{g,NO_3} were plotted against particle diameter d_p in Fig. 2. Diffusion effect becomes larger at larger d_p.

5   The flux of adsorption of gas molecules on the quasi-static particle surface can be expressed as

$$J_{ads,X_i} = \alpha_{s,X_i} J_{coll,X_i} = k_{a,X_i}[X_i]_{gs} \tag{5}$$

where α_{s,X_i} is surface accommodation coefficient and k_{a,X_i} ($=\alpha_{s,X_i}\varpi_{X_i}/4$) is a first-order adsorption rate coefficient. In Langmuir adsorption model, α_{s,X_i} is determined
10 by the surface accommodation coefficient on an adsorbate-free surface $\alpha_{s,0,X_i}$ and the sorption layer coverage θ_s, which is given by the sum of the fractional surface coverage of all competing adsorbate species (i.e. O_3, H_2O, and NO_2) θ_{s,X_p}.

$$\alpha_{s,X_i} = \alpha_{s,0,X_i}(1 - \theta_s) = \alpha_{s,0,X_i}(1 - \sum \theta_{s,X_p}) \tag{6}$$

θ_{s,X_p} is the ratio of surface concentration of X_p and concentration of surface sorption
15 site $[SS]_{ss}$: $\theta_{s,X_p}=[X_p]_s/[SS]_{ss}$. Surface sorption site $[SS]_{ss}$ is the inverse of the effective molecular cross section of X_p, σ_{s,X_p}. In this study, we assume $[SS]_{ss}$ is independent on adsorbate gas of O_3, H_2O, and NO_2 (i.e. $\sigma_{s,O_3}=\sigma_{s,H_2O}=\sigma_{s,NO_2}$).

The adsorbed molecules can thermally desorb back to the gas phase. Desorption, the inverse of adsorption, can be described by a first-order rate coefficient k_{d,X_i}, which
20 is assumed to be independent on θ_{s,X_i}. The flux of desorption of gas molecules on the quasi-static particle surface can be expressed as

$$J_{des,X_i} = k_{d,X_i}[X_i]_s = \tau_{d,X_i}^{-1}[X_i]_s \tag{7}$$

The desorption lifetime τ_{d,X_i} is the mean residence time on the surface in the absence of surface reaction and surface-bulk transport. Since molecules are desorbed ther-

mally, k_{d,X_i} depends strongly on temperature. This can be described by an Arrhenius equation as described below.

$$k_{d,X_i} = A \exp(\Delta H_{ads,X_i}/RT) \tag{8}$$

A pre-exponential factor A is typically $\sim 10^{14}\,s^{-1}$ for chemisorbed species, which is approximately the vibrational frequency of a molecule bound to the surface. For physisorbed species, A is typically $\sim 10^{12}\,s^{-1}$. Adsorption enthalpy of gaseous X_i, $\Delta H_{ads,X_i}$ can be estimated roughly by assuming A.

The uptake coefficient of gas species X_i can be expressed as a ratio between the net fluxes of X_i from the gas phase to the condensed phase J_{net,X_i}, and J_{coll,X_i}.

$$\gamma_{X_i} = \frac{J_{net,X_i}}{J_{coll,X_i}} = \frac{J_{ads,X_i} - J_{des,X_i}}{J_{coll,X_i}} \tag{9}$$

2.2 Surface layer reactions (Langmuir-Hinshelwood-type mechanism)

The surface layer reactions (SLRs) occur within the surface double layer and involve only adsorbed species or components of the quasi-static layer. In this study the PAH-O_3 system is considered to follow a Langmuir-Hinshelwood-type mechanism, in which ozone first adsorbs to the surface and then reacts with PAH in a quasi-static surface layer (Pöschl et al., 2001; Ammann et al., 2003; Ammann and Pöschl, 2007; Pöschl et al., 2007). Note, however, that traditionally the term "Langmuir-Hinshelwood mechanism" is used for surface catalytic reactions between adsorbed gas species and not to describe reactions that transform the surface (Masel, 1996; IUPAC, 1997). Here we consider three SLRs:

$$PAH(ss) + O_3(s) \rightarrow o1\text{-}PAH(ss) \tag{SLR1}$$
$$O_3(s) + NO_2(s) \rightarrow NO_3(s) \tag{SLR2}$$
$$PAH(ss) + NO_3(s) \rightarrow o2\text{-}PAH(ss) \tag{SLR3}$$

The products of SLR1 and SLR3, o1-PAH and o2-PAH, are oxidized non-volatile PAHs. The surface reaction of O_3 and NO_2 produces the highly reactive NO_3 radical, which can react with PAH immediately. The degradation rate of PAH ($L_{SLR,PAH}$) can be described using the second-order rate coefficients k_{SLR,PAH,O_3} and k_{SLR,PAH,NO_3},

$$L_{SLR,PAH} = k_{SLR,PAH,O_3}[PAH]_{ss}[O_3]_s + k_{SLR,PAH,NO_3}[PAH]_{ss}[NO_3]_s = k_{s,PAH}[PAH]_{ss} \tag{10}$$

where $k_{s,PAH}$ ($=k_{SLR,PAH,O_3}[O_3]_s + k_{SLR,PAH,NO_3}[NO_3]_s$) is an apparent first-order PAH decay rate coefficient.

The loss rate of ozone by SLR1-SLR2 (L_{SLR,O_3}) can be described as

$$L_{SLR,O_3} = k_{SLR,PAH,O_3}[PAH]_{ss}[O_3]_s + k_{SLR,O_3,NO_2}[O_3]_s[NO_2]_s = k_{s,O_3}[O_3]_s \tag{11}$$

where k_{s,O_3} ($=k_{SLR,PAH,O_3}[PAH]_{ss} + k_{SLR,O_3,NO_3}[NO_2]_s$) is an apparent first-order ozone loss rate coefficient.

The production rate of NO_3 on the surface, P_{SLR,NO_3}, can be described as

$$P_{SLR,NO_3} = k_{SLR,O_3,NO_2}[O_3]_s[NO_2]_s - k_{SLR,PAH,NO_3}[PAH]_{ss}[NO_3]_s \tag{12}$$

2.3 Gas-surface reaction (Eley-Rideal-type mechanism)

The gas-surface reaction is a single kinetic step of collision and reaction between gaseous species and surface molecules, which can be regarded as an Eley-Rideal-type mechanism (Ammann and Pöschl, 2007; Pöschl et al., 2007). Note that traditionally the term "Eley-Rideal mechanism" (also named Rideal-Eley or Langmuir-Rideal mechanism) is used for surface catalytic reaction between adsorbed gas species rather than for reactions that transform the surface (Masel, 1996; IUPAC, 1997). Here we consider two GSRs.

$$PAH(ss) + OH(gs) \rightarrow o3\text{-}PAH(ss) \tag{GSR1}$$
$$PAH(ss) + NO_3(gs) \rightarrow o4\text{-}PAH(ss) \tag{GSR2}$$

Heterogeneous loss of PAH on the surface ($L_{GSR,PAH}$) can be described by the following equation (Pöschl et al., 2007).

$$L_{GSR,PAH} = \sum_{X_i} \gamma_{GSR,X_i,PAH} \theta_{SS,PAH}(1 - \theta_S) J_{coll,X_i} \tag{13}$$

Here $\gamma_{GSR,X_i,PAH}$ is defined as the elementary surface reaction probability that X_i (OH or NO_3) undergoes gas-surface reaction when colliding with PAH on the surface. $\theta_{ss,PAH}$ is the surface coverage of PAH.

2.4 Steady-state conditions

The surface mass balance and rate equations can be described as below in summary (Pöschl et al., 2007).

$$d[O_3]_s/dt \quad = J_{ads,O_3} - J_{des,O_3} - L_{SLR,O_3} \tag{14}$$
$$d[H_2O]_s/dt \quad = J_{ads,H_2O} - J_{des,H_2O} \tag{15}$$
$$d[NO_2]_s/dt \quad = J_{ads,NO_2} - J_{des,NO_2} - L_{SLR,NO_2} \tag{16}$$
$$d[PAH]_{ss}/dt = -L_{SLR,PAH} - L_{GSR,PAH} \tag{17}$$
$$d[NO_3]_s/dt \quad = P_{SLR,NO_3} - J_{des,NO_3} \tag{18}$$

Steady-state conditions are characterized by $d[X_i]_s/dt = 0$ ($X_i = O_3$, H_2O, and NO_2). The effective Langmuir adsorption equilibrium constant K'_{ads,X_i} can be described as below.

$$K'_{ads,X_i}[X_i]_{gs} = \frac{\theta_{s,X_i}}{1 - \theta_s} \tag{19}$$

$$K'_{ads,X_i} = \sigma_{s,X_i} \frac{k_{a,0,X_i}}{k_{d,X_i} + k_{s,X_i}} \tag{20}$$

If surface reactions are much slower than desorption ($k_{d,X_i} \gg k_{s,X_i}$), then K'_{ads,X_i} is equal to a Langmuir adsorption equilibrium constant K_{ads,X_i} ($= \sigma_{s,X_i} k_{a,0,X_i}/k_{d,X_i}$). Under these

conditions the desorption lifetime τ_{d,X_i} and first-order rate coefficient k_{d,X_i} are given by

$$k_{d,X_i} = \frac{1}{\tau_{d,X_i}} \approx \sigma_{s,X_i} \frac{k_{a,0,X_i}}{K'_{ads,X_i}} = \frac{\alpha_{s,0,X_i} \omega_{X_i} \sigma_{s,X_i}}{4K'_{ads,X_i}} \tag{21}$$

The surface concentration of X_i can be expressed as

$$[X_i]_s = [SS]_{ss}\theta_{s,X_i} = [SS]_{ss} \frac{K'_{ads,X_i}[X_i]_{gs}}{1 + \sum K'_{ads,X_i}[X_i]_{gs}} \tag{22}$$

An apparent first order rate coefficient $k_{s,PAH}$ can be described as

$$k_{s,PAH} = k_{s,PAH,max} \frac{K'_{ads,X_i}[X_i]_{gs}}{1 + \sum_p K'_{ads,X_p}[X_p]_{gs}} \tag{23}$$

where $k_{s,PAH,max}$ is a maximum pseudo-first order rate coefficient of PAH.

The uptake coefficient of ozone (γ_{O_3}) can be calculated as

$$\gamma_{O_3} = \frac{L_{SLR,O_3}}{J_{coll,O_3}} = \frac{4k_{s,PAH}}{\sigma_{PAH}\omega_{O_3}[O_3]_{gs}} \tag{24}$$

The initial concentration of PAH is considered to be the inverse of the effective molecular cross section σ_{PAH} and is estimated assuming one aromatic ring has $0.2\,nm^2$. For example, σ_{BaP} is assumed to be $1\,nm^2$ because BaP consists of five aromatic rings (Pöschl et al., 2001).

3 Experimental data analysis and steady-state condition

3.1 PAH-O$_3$-H$_2$O system

The kinetics of the heterogeneous reaction between PAHs bound on a substrate and gas phase ozone were investigated in various laboratory studies (Wu et al., 1984;

Alebic-Juretic et al., 1990; Pöschl et al., 2001; Ammann et al., 2003; Mmereki and Donaldson, 2003; Kwamena et al., 2004, 2006, 2007; Mmereki et al., 2004; Donaldson et al., 2005; Kahan et al., 2006). The investigated PAHs in this current study are benzo[a]pyrene (BaP), anthracene, naphthalene, pyrene, phenanthrene,
5 benzo[a]anthracene (BaA), perylene, and fluoranthene. Degradation kinetics of a self-assembled monolayer (SAM) of alkenes and cypermethrin were also analyzed as references (Dubowski et al., 2004; Segal-Rosenheimer and Dubowski, 2008), as they were also observed to follow a Langmuir-Hinshelwood-type mechanism. The heterogeneous reactions between PAH with ozone were investigated for a wide range of substrates,
10 including aerosols of soot, azelaic acid and phenylsiloxane oil, and solid and liquid of glass, ZnSe, non-activated silica gel, fused silica, and water, octanol, decanol, stearic aicd, octanoic acid, and hexanoic acid, respectively.

3.1.1 Basic physicochemical parameters

A pseudo-first order rate PAH decay coefficient ($k_{s,PAH}$) was reported by laboratory
15 studies as a function of gas phase ozone concentration as shown in Fig. 3. They showed nonlinear relationship with a shape that is consistent with the Langmuir-Hinshelwood-type mechanism. This is in contrast to Eley-Rideal-type mechanism, which would display a linear dependence of $k_{s,PAH}$ on gas phase ozone concentration.
   A non-linear least-square fit to the experimental data pairs of $k_{s,PAH}$ and $[O_3]_{gs}$ for
20 each substrate is displayed in Fig. 3. In PAH-O_3-H_2O system Eq. (23) can be simplified to

$$k_{s,PAH} = k_{s,PAH,max} \frac{K'_{ads,O_3}[O_3]_{gs}}{1 + K'_{ads,O_3}[O_3]_{gs} + K'_{ads,H_2O}[H_2O]_{gs}} \qquad (25)$$

The fit parameters of $k_{s,PAH,max}$ and K'_{ads,O_3} are obtained by fitting to data using Eq. (25) and summarized in Table 1. Pöschl et al. (2001) measured the surface concentration
25 of ozone, $[O_3]_s$, as a function of gas phase ozone concentration, which can be fitted by

following equation.

$$[O_3]_s = [SS]_{ss} \frac{K'_{ads,O_3}[O_3]_{gs}}{1 + K'_{ads,O_3}[O_3]_{gs} + K'_{ads,H_2O}[H_2O]_{gs}} \qquad (26)$$

A non-linear square fit of these data leads to $[SS]_{ss}=5.8\times10^{14}\,cm^{-2}$ ($\sigma_{s,O_3}=0.17\,nm^2$). We assumed this value for the other studies as well because as Pöschl et al. (2001) is the only study that measured $[O_3]_s$. A second-order rate coefficient (k_{SLR,PAH,O_3}) can be calculated using the relation $k_{s,PAH,max}=k_{SLR,PAH,O_3}[SS]_{ss}$. The desorption lifetime of O_3 on the surface (τ_{d,O_3}) and desorption rate coefficients (k_{d,O_3}) were estimated using Eq. (21), assuming the surface accommodation coefficient on an adsorbate-free surface ($\alpha_{s,0,O_3}$) of 1.0×10^{-3} (Rogaski et al., 1997).

The τ_{d,O_3} was calculated to be in the range of 10 ms–10 s depending on substrate materials. The relatively longer desorption lifetime and the fact that the experimental data can be described by Langmuir adsorption suggest chemisorption of O_3 – possibly in the form of O atom – rather than physisorption. The adsorption enthalpy $\Delta H_{ads,O_3}$ was roughly estimated using Eq. (8), assuming a pre-exponential factor (A) of $10^{14}\,s^{-1}$. We calculated $\Delta H_{ads,O_3}$ with $A=10^{12}$–$10^{15}\,s^{-1}$, this leads to an uncertainty of $\pm6\,kJ\,mol^{-1}$ in $\Delta H_{ads,O_3}$. K'_{ads,O_3} is approximated to K_{ads,O_3}, as k_{d,O_3} is one to three orders of magnitude larger than $k_{s,O3}$. K_{ads,O_3} are one to three orders of magnitude larger on a solid substrate compared to on a liquid substrate. This leads to a longer desorption lifetime and higher $\Delta H_{ads,O_3}$ ($\approx-(70-90)\,kJ\,mol^{-1}$) on a solid substrate. Additionally, $k_{s,PAH,max}$ and k_{SLR,PAH,O_3} are factor of 10 larger on a solid substrate compared to a liquid one. Note that self-assembled monolayer of alkenes showed similar adsorption and reaction rate values as PAH, whereas cypermethrin showed significant lower reaction rate.

The surface kinetics were also investigated at a relative humidity of 25% (Pöschl et al., 2001) and 72% (Kwamena et al., 2004), respectively. The K_{ads,H_2O} for these conditions are summarized in Table 2. The K_{ads,H_2O} values are on the order of $10^{-17}\,cm^{-3}$,

Full Screen / Esc

Printer-friendly Version

Interactive Discussion

which are 2–4 orders of magnitude smaller than K_{ads,O_3}. $\alpha_{s,0,H_2O}$ of 6.0×10^{-4} (Rogaski et al., 1997) was assumed in order to estimate τ_{d,H_2O} and k_{d,H_2O}. The desorption lifetime of H_2O (τ_{d,H_2O}) was ca. 50 ms, indicating the physisorption of H_2O. The adsorption enthalpy $\Delta H_{ads,H_2O}$ was estimated to be $-36(\pm9)$ kJ mol^{-1} assuming a range
5 of pre-exponential factor values (10^8–10^{12} s^{-1}).

3.1.2 Uptake of ozone

The γ_{O_3} values of the PAH-O_3-H_2O system were calculated using Eq. (24) and are shown in Fig. 4. The γ_{O_3} values showed a strong $[O_3]_{gs}$ dependence over five orders of magnitude ($[O_3]_{gs}\approx10$–10^6 ppb). The curves are modeled using K2-SURF assuming
10 three cases; 1) $\tau_{d,O_3}=10$ s, $k_{SLR,PAH,O_3}=2.7\times10^{-17}$, on a soot surface (Fig. 4, red solid line), 2) $\tau_{d,O_3}=1$ s, $k_{SLR,PAH,O_3}=2.7\times10^{-17}$, on a solid organic surface (red dotted line), 3) $\tau_{d,O_3}=0.1$ s, $k_{SLR,PAH,O_3}=5.0\times10^{-18}$, on a liquid surface (black solid line). Systems on a solid substrate such as soot, glass and solid organic substrate are explained very well by the red lines in Fig. 4, over five orders of magnitude. As can be seen in Fig. 4,
15 most experimental data are obtained at high $[O_3]_{gs}$ range. The γ_{O_3} can be extrapolated to atmospheric condition ($[O_3]_{gs}<150$ ppb) by the modeled lines. The γ_{O_3} of PAH on a soot surface is estimated to be $(1$–$3)\times10^{-5}$ and $\sim10^{-6}$ on a solid organic surface.

The γ_{O_3} on a liquid octanol surface (triangle markers in Fig. 4) showed significantly lower values compared to the γ_{O_3} on a solid surface. One possible explanation is
20 that some PAH was dissolved into the octanol so the actual PAH concentration on the surface was decreased leading to the reduction of γ_{O_3} based on Eq. (24). The transport of PAH from quasi-static layer to bulk can be modelled using surface-bulk mass transport fluxes $J_{ss,b}$, which is beyond the present study. Still, these data are well fitted by black solid line ($\tau_{d,O_3}=0.1$ s, $k_{SLR,PAH,O_3}=5.0\times10^{-18}$), which suggests γ_{O_3}
25 at atmospheric condition in the order of 10^{-8}.

3.2 PAH-O$_3$-H$_2$O-NO$_2$ system

The oxidation of PAH upon interactions with O$_3$, H$_2$O and NO$_2$ were investigated using data from Schauer (2004). A pseudo-first order PAH decay rate coefficient ($k_{s,PAH}$) and the surface concentration of ozone, $[O_3]_s$, were measured as a function of gas phase ozone concentration as shown in Fig. 5, which can be fitted by following equations.

$$[O_3]_s = [SS]_{ss} \frac{K'_{ads,O_3}[O_3]_{gs}}{1 + K'_{ads,O_3}[O_3]_{gs} + K'_{ads,H_2O}[H_2O]_{gs} + K'_{ads,NO_2}[NO_2]_{gs}} \quad (27)$$

$$k_{s,PAH} = k_{s,PAH,max} \frac{K'_{ads,O_3}[O_3]_{gs}}{1 + K'_{ads,O_3}[O_3]_{gs} + K'_{ads,H_2O}[H_2O]_{gs} + K'_{ads,NO_2}[NO_2]_{gs}} \quad (28)$$

Using these equations of the non-linear fit, the K'_{ads,NO_2} was estimated, which are summarized in Table 3. The K'_{ads,NO_2} values are on the order of 10^{-14} cm^3, which are comparable to K_{ads,O_3}. The τ_{d,NO_2} values were estimated to be ca. 50 ms, indicating the chemisorption of NO$_2$. The adsorption enthalpy $\Delta H_{ads,NO_2}$ was estimated to be $-67(\pm 6)$ kJ mol^{-1} assuming a range of pre-exponential factors ($A \approx 10^{12}$–10^{14} s^{-1}).

Table 4 shows the basic physicochemical parameters of O$_3$ in this system. The sorption sites decrease systematically as NO$_2$ concentration increases, which implies that the effective molecular cross section of ozone (or O atom) is smaller than that of NO$_2$ ($\sigma_{s,O_3}(\sigma_{s,O}) < \sigma_{s,NO_2}$). The apparent k_{SLR,PAH,O_3} was estimated assuming $k_{SLR,O_3,NO_2} = 0$. It is interesting to note that $k_{s,PAH,max}$ and k_{SLR,PAH,O_3} increase systematically as NO$_2$ concentration increase. For example, k_{SLR,PAH,O_3} increases from 2.66×10^{-17} cm^2 s^{-1} to 5.70×10^{-17} cm^2 s^{-1}, when NO$_2$ increases from 0 to 500 ppb, which indicates the acceleration of PAH degradation. The PAH degradation was not observed when PAHs are exposed to only NO$_2$ with concentrations of up to 1 ppm, which means NO$_2$ alone does not efficiently degrade PAHs (Schauer et al., 2003). Therefore, the accelerating effect of NO$_2$ can be attributed to the formation of the highly reactive NO$_3$ radicals

Title Page

Abstract | Introduction

Conclusions | References

Tables | Figures

◀◀ | ▶▶

◀ | ▶

Back | Close

Full Screen / Esc

Printer-friendly Version

Interactive Discussion

formed in gas phase or on the surface, or other reactive nitrogen species like N_2O_5 or HNO_3. The reactive uptake coefficients of N_2O_5 or HNO_3 are reported to be below $\sim 10^{-5}$, therefore they are unlikely to react with PAHs at ambient conditions (Gross and Bertram, 2008).

4 Numerical modeling of transient conditions

Here we model the temporal evolution of surface composition and uptake coefficients of ozone over timescales from microseconds to days under standard conditions (298 K, 1013 hPa). The simulations were performed by solving the rate equations (Eqs. 14–18) numerically with a Matlab program.

The initial concentration of PAH is set to be 1×10^{14} cm^{-2}, and the initial surface concentration of gas species (O_3, H_2O, NO_2, and NO_3) is 0. For the exemplary model simulations, we consider PAH degradation both on soot and organics surface. The basic physicochemical parameters required in the simulations are the surface accommodation coefficient on the free substrate ($\alpha_{s,0}$), the mean thermal velocity of gases (ω), the desorption lifetime of species (τ_d), and the second-order rate coefficient (k_{SLR,PAH,O_3}), which are summarized in Table 5. The $\alpha_{s,0}$ values were taken from previous studies (Tabor et al., 1994; Rogaski et al., 1997). The τ_d and k_{SLR,PAH,O_3} were determined based on Sect. 3. The gas phase O_3 concentration is set to be 100 ppb, which is typical ozone concentration in polluted air mass. The chemical half-life of PAH on the surface ($t_{1/2}$) is estimated, which is defined as the time when the PAH concentration reaches half of the initial concentration.

4.1 PAH-O_3-H_2O system

Here we modeled PAH degradation upon interactions with O_3 and H_2O. Figure 6 shows the surface concentrations of all involved chemical species and the uptake coefficient of O_3 (γ_{O_3}). We modeled PAH degradation on soot surface under dry (0% RH) and wet

conditions (25% RH). Figure 6a shows the results at 25% RH. The initial plateau of γ_{O_3} is equal to $\alpha_{s,0,O_3}$ ($=10^{-3}$) up to 1 s, which can be explained as adsorption of O_3 onto an adsorbate free surface. The second plateau of γ_{O_3} at $\sim 10^{-5}$ is due to chemical reaction of O_3 with PAH. The temporal evolutions of surface species at 25% RH are analogous

5 under dry conditions (not shown in figure), except that the competitive adsorption of H_2O has the following consequences: (a) the surface coverage of O_3 becomes lower at 25% RH due to competitive adsorption of O_3 and H_2O, (b) the PAH chemical half-life increased from 168 s (dry) to 188 s (25% RH).

When PAH is on the organics surface with τ_{d,O_3} of 0.1 s, the dominant species on

10 the surface is H_2O and the maximum surface coverage of O_3 reaches only 0.1% in a short time (ca. 0.1 s) as shown in Fig. 6b. Consequently, the second plateau of γ_{O_3} is largely extended to $\sim 10^4$ s due to slow PAH degradation. Additionally, the second plateau value of γ_{O_3} is lower on the organics ($\gamma_{O_3} \sim 10^{-7}$) than on the soot ($\gamma_{O_3} \sim 10^{-5}$).

4.2 PAH-O_3-H_2O-OH system

15 We modeled PAH degradation by O_3, H_2O, and OH. Here we assume that the reported γ_{OH} of 0.32 (Bertram et al., 2001) is equal to elementary surface reaction probabilities $\gamma_{GSR,OH,PAH}$. OH radicals colliding with PAH are assumed to react immediately due to the OH radical's high reactivity. The near-surface gas phase concentration of OH was corrected using a gas phase diffusion correction factor ($C_{g,OH}$) of 0.87 and

20 assuming a particle diameter of 200 nm. The two dotted lines in Fig. 6a and b correspond to two different OH concentrations: a globally averaged ambient concentration ($[OH]_g=1\times10^6\,cm^{-3}$) (Prinn et al., 1992) and an approximate upper limits in polluted air ($[OH]_g=1\times10^7\,cm^{-3}$).

Figure 6a shows that OH does not affect PAH degradation on soot significantly. In

25 this case O_3 plays the dominant role in the PAH degradation. On the other hand, OH largely accelerates PAH degradation on an organic surface as shown in Fig. 6b. As a consequence, the plateau of γ_{O_3} is an order of magnitude shorten depending on OH

Title Page

Abstract | Introduction

Conclusions | References

Tables | Figures

◄ | ►

◄ | ►

Back | Close

Full Screen / Esc

Printer-friendly Version

Interactive Discussion

concentration. Therefore OH plays a main role in PAH degradation on an organics surface.

4.2.1 PAH chemical half-life on the surface and atmospheric implications

We have estimated the chemical half-life of PAH ($t_{1/2}$) on soot, organic and liquid sur-
faces, when exposed to ambient concentrations of O_3 and OH and with a RH=25%.
   Figure 7 displays the results of these calculations. The black line is the $t_{1/2}$ of PAH
on a soot surface at 25% RH, which showed $t_{1/2}$ of ~10 min at typical atmospheric
O_3 concentration of 30 ppb. We calculated $t_{1/2}$ under dry conditions as well, which
resulted in a $t_{1/2}$ value of ~5 min at 30 ppb O_3. Therefore, the competitive adsorption
of O_3 and H_2O leads to a significant increase in $t_{1/2}$. However, the $t_{1/2}$ values showed
only a slight change with increasing $[OH]_g$. This is because PAH degradation on soot
is dominated by the surface layer reaction of PAH with O_3.
   The $t_{1/2}$ values on a solid organic surface (Fig. 7, red and blue line) are estimated
to be 2–15 h at 30 ppb O_3 when the OH concentration is 0. The $t_{1/2}$ value on a liquid
organic surface like octanol (green line) is estimated to be a few days. As shown in
Fig. 7, τ_{d,O_3} is a critical factor in estimating the chemical half-life of PAH on the surface.
OH plays a critical role in these cases. It accelerates the PAH degradation by one to
two orders of magnitude depending on OH concentration.
   In summary, the PAH chemical half-life on the surface ($t_{1/2}$) ranges from ~10 min on
soot, to 1–5 h on solid organics and 6 h on liquid particles under typical ambient condi-
tions (30 ppb O_3, 25% RH, 10^6 cm^{-3} OH). The relative importance of PAH degradation
by O_3 and OH depends on the substrate of PAH.

4.3 PAH-O_3-H_2O-NO_2-NO_3 system

Here we modeled PAH degradation on soot upon interactions with O_3, H_2O, NO_2, and
NO_3. As discussed in Sect. 4.1, if other gas species (i.e. H_2O) coexist with ozone in
the system, competitive adsorption leads to slower degradation. Therefore, if we con-

sider neither the surface reaction of O_3 with NO_2 nor gas-surface reaction of NO_3, then competitive adsorption of NO_2 leads to slower PAH degradation. This is inconsistent with experimental results (Table 4), which shows that NO_2 accelerates PAH degradation. For example, the apparent k_{SLR,PAH,O_3} is increased from $2.7 \times 10^{-17}\,\mathrm{cm^2\,s^{-1}}$ to $5.7 \times 10^{-17}\,\mathrm{cm^2\,s^{-1}}$ (Table 4) under 500 ppb NO_2, leading to a reduction of $t_{1/2}$ from 188 s to 170 s at 100 ppb O_3 and 25% RH. Here we considered two possible explanations for the acceleration of PAH degradation: (1) surface reaction of O_3 with NO_2 (Langmuir-Hinshelwood-type mechanism) and (2) gas-surface reaction between PAH and gas phase NO_3 radical (Eley-Rideal-type mechanism).

4.3.1 Surface reaction of O_3 with NO_2

We modeled the PAH-O_3-H_2O-NO_2-soot system considering a surface reaction of O_3 with NO_2 (SLR2) and the subsequent reaction of NO_3 with PAH (SLR3). We tested k_{SLR,O_3,NO_2} and k_{SLR,PAH,NO_3} values in the range of 10^{-18}–$10^{-11}\,\mathrm{cm^2\,s^{-1}}$. The desorption lifetime of NO_3 (τ_{d,NO_3}) was assumed to be 10 and 0.01 s. The concentrations of O_3 and NO_2 at 25% RH are set at 100 and 500 ppb, respectively. The resulting PAH chemical half-lifes ($t_{1/2}$) are summarized in Table 6.

The $t_{1/2}$ value should be ~170 s considering the acceleration of PAH degradation. Moreover, the fact that the PAH-O_3-H_2O-NO_2 system is well described by Langmuir-Hinshelwood-type mechanism (Fig. 5) indicates $L_{SLR,O_3} \ll J_{des,O_3}$, leading to k_{s,O_3} $(=k_{SLR,PAH,O_3}[PAH]_{ss}+k_{SLR,O_3,NO_2}[NO_2]_s) \ll k_{d,O_3}$. Considering k_{d,O_3} is ~10^{-1} and $[NO_2]_s$ and $[PAH]_{ss}$ is ~10^{14}, then k_{SLR,O_3,NO_2} should be $<10^{-16}$.

Based on these criteria, k_{SLR,O_3,NO_2} should be on the order of 10^{-17}–$10^{-16}\,\mathrm{cm^2\,s^{-1}}$, whereas k_{SLR,PAH,NO_3} is on the order of 10^{-15}–$10^{-12}\,\mathrm{cm^2\,s^{-1}}$. This is reasonable because k_{SLR,O_3,NO_2} is on the same order of k_{SLR,PAH,O_3} and the NO_3 radical is expected to have high reactivity. The possible combination of rate coefficients are 1) $\tau_{d,NO_3}=10$ s, $k_{SLR,O_3,NO_2}=10^{-17}$–$10^{-16}\,\mathrm{cm^2\,s^{-1}}$, $k_{SLR,PAH,NO_3}=10^{-15}$–$10^{-14}\,\mathrm{cm^2\,s^{-1}}$

and 2) $\tau_{d,NO_3}=0.01$ s, $k_{SLR,O_3,NO_2}=10^{-17}-10^{-16}$ cm^2 s^{-1}, $k_{SLR,PAH,NO_3}=10^{-13}-10^{-12}$ cm^2 s^{-1}.

Figure 8a shows the exemplary simulation of this system using $\tau_{d,NO_3}=10$ s, $k_{SLR,O3,NO2}=10^{-17}$ cm^2 s^{-1}, and $k_{SLR,PAH,NO3}=10^{-14}$ cm^2 s^{-1}. Temporal evolution is similar to Fig. 6a, but the PAH degradation was accelerated by formation of NO$_3$ radical, whose concentration reaches $\sim 10^{12}$ cm^{-2}. The uptake coefficient of O$_3$ (γ_{O_3}) stayed 10^{-5} because of continuous surface reaction of O$_3$ with NO$_2$.

4.3.2 Gas-surface reaction with NO$_3$

Gas-surface reaction between gas phase NO$_3$ and PAH is another possible explanation for the acceleration of PAH degradation. This system corresponds to a possible nighttime chemistry of PAH degradation, as NO$_3$ is the dominant oxidant at nighttime. The degradation of PAHs on a soot surface when exposed to O$_3$, H$_2$O, NO$_2$, and gas phase NO$_3$ was modeled in Fig. 8b. Note that the surface reaction of O$_3$ with NO$_2$ is not considered in this simulation. The NO$_3$ reactive uptake coefficient by PAH is reported to be 0.13 (Rudich et al., 1996). We assumed this is equal to the elementary surface reaction probability $\gamma_{GSR,NO_3,PAH}$. The near-surface gas phase concentration of NO$_3$ was corrected by the gas phase diffusion correction factor (C_{g,NO_3}) of 0.94 and assuming a particle diameter of 200 nm (Fig. 2). The concentration of O$_3$ and NO$_2$ at 25% RH are set to be 100 ppb and 500 ppb, respectively. Four NO$_3$ concentrations that cover the range of ambient concentrations (1, 10, 20, and 100 ppt) were assumed (Finlayson-Pitts and Pitts, 2000).

When the NO$_3$ concentration is 1 ppt, the presence of NO$_3$ does not impact the degradation of PAHs significantly, but rather ozone plays a dominant role in PAH degradation. The NO$_3$ radicals compensate the competitive adsorption of NO$_2$ when NO$_3$ concentration is 10 ppt with $t_{1/2}$ of 186 s. The $t_{1/2}$ is 144 s when the NO$_3$ concentration is 20 ppt. And for 100 ppt NO$_3$ concentration, the $t_{1/2}$ is calculated to be 38 s, which means the PAH degradation is dominated by the NO$_3$ radical at this condition.

Printer-friendly Version

Interactive Discussion

4.3.3 PAH chemical half-life on the surface and atmospheric implications

The chemical half-life ($t_{1/2}$) of PAH on the surface (soot, organics, and liquid) was estimated upon interactions with O_3, H_2O, NO_2, and NO_3 at ambient concentration level (<150 ppb O_3, 25% RH, 100 ppb NO_2, 1–10 ppt NO_3). Figure 9 displays the
5 results of calculations. Neither the surface reaction of O_3 with NO_2 nor gas-surface reaction of NO_3 was considered for the thick solid line. NO_3 accelerates the PAH degradation by one to three orders of magnitude depending on NO_3 concentration (Fig. 9, dotted and dashed line). The surface reaction of O_3 and NO_2 decreases the $t_{1/2}$ by ca. 40% on every surface (Fig. 9, solid line).
10   In summary, under typical ambient conditions at night time (i.e. 30 ppb O_3, 100 ppb NO_2, 25% RH, 1 ppt NO_3), the PAH chemical half-life on the surface ($t_{1/2}$) ranges from ~10 min on soot, to 30–60 min on solid organics and liquid particles. The NO_3 radical can degrade PAH and $t_{1/2}$ depends largely on NO_3 concentration.

5 Conclusions

15 We have developed and applied a kinetic double-layer surface model (K2-SURF) and chemical reaction mechanism to describe the degradation of polycyclic aromatic hydrocarbons (PAHs) on aerosol particles interacting with ozone, nitrogen dioxide, water vapor, hydroxyl and nitrate radicals. Basic physicochemical parameters have been derived from experimental data and used to simulate PAH degradation and ozone uptake
20 by aerosol particles under a wide range of conditions. The main conclusions are:

   1. The heterogeneous reaction between particle-bound PAHs and ozone can be well described by Langmuir-Hinshelwood-type mechanism and rate equations with effective Langmuir adsorption constants and surface reaction rate coefficients depending on the substrate material.

25   2. Competitive and reversible adsorption and chemical transformation of the surface

(aging) lead to a strong non-linear dependence of the ozone uptake coefficients on time and gas phase composition with different characteristic features under dilute atmospheric and concentrated laboratory conditions. Under typical ambient conditions the ozone uptake coefficients of PAH-coated aerosol particles are likely in the range of 10^{-6}–10^{-5}.

3. Nitrogen dioxide undergoes competitive co-adsorption with ozone. At ambient temperatures NO_2 alone does not efficiently degrade PAHs, but it can accelerate PAH degradation by ozone. The accelerating effect of NO_2 can be explained by the formation of highly reactive NO_3 radicals in the gas phase and on the surface.

4. The chemical half-life of PAH is expected to range from a few minutes on the surface of soot, to multiple hours on solid organics and days on liquid particles. On soot, PAH degradation appears to be dominated by a surface layer reaction with adsorbed O_3 (Langmuir-Hinshelwood-type mechanism). On other substrates, it seems to be dominated by gas-surface reaction with OH and NO_3 radicals (Eley-Rideal-type mechanism).

5. To our knowledge, K2-SURF is the first atmospheric process model describing multiple types of parallel and sequential surface reactions between multiple gaseous and particle-bound chemical species. We suggest that it may serve as a basis for the development of a general master mechanism of aerosol and cloud surface chemistry, and we intend to pursue this development in follow-up studies including other organic aerosol components.

Kinetic double layer model (K2-SURF)

M. Shiraiwa et al.

References

Ackerman, A. S., Toon, O. B., Stevens, D. E., Heymsfield, A. J., Ramanathan, V., and Welton, E. J.: Reduction of tropical cloudiness by soot, Science, 288(5468), 1042–1047, 2000.

Alebic-Juretic, A., Cvitas, T., and Klasinc, L.: Heterogeneous polycyclic aromatic hydrocarbon degradation with ozone on silica-gel carrier, Environ. Sci. Technol., 24(1), 62–66, 1990.

Ammann, M. and Pöschl, U.: Kinetic model framework for aerosol and cloud surface chemistry and gas-particle interactions – Part 2: Exemplary practical applications and numerical simulations, Atmos. Chem. Phys., 7(23), 6025–6045, 2007.

Ammann, M., Pöschl, U., and Rudich, Y.: Effects of reversible adsorption and Langmuir-Hinshelwood surface reactions on gas uptake by atmospheric particles, Phys. Chem. Chem. Phys., 5, 351–356, 2003.

Andreae, M. O. and Rosenfeld, D.: Aerosol-cloud-precipitation interactions. Part 1. The nature and sources of cloud-active aerosols, Earth-Sci. Rev., 89(1–2), 13–41, 2008.

Atkinson, R. and Arey, J.: Atmospheric chemistry of gas-phase polycyclic aromatic-hydrocarbons – formation of atmospheric mutagens, Environ. Health Persp., 102, 117–126, 1994.

Bertram, A. K., Ivanov, A. V., Hunter, M., Molina, L. T., and Molina, M. J.: The reaction probability of OH on organic surfaces of tropospheric interest, J. Phys. Chem. A, 105(41), 9415–9421, 2001.

Donaldson, D. J., Mmereki, B. T., Chaudhuri, S. R., Handley, S., and Oh, M.: Uptake and reaction of atmospheric organic vapours on organic films, Faraday Discuss., 130, 227–239, 2005.

Dubowski, Y., Vieceli, J., Tobias, D. J., Gomez, A., Lin, A., Nizkorodov, S. A., McIntire, T. M., and Finlayson-Pitts, B. J.: Interaction of gas-phase ozone at 296 K with unsaturated self-assembled monolayers: A new look at an old system, J. Phys. Chem. A, 108(47), 10473–10485, 2004.

Finlayson-Pitts, B. J. and Pitts, J. N. (Eds.): Chemistry of the Upper and Lower Atmosphere, Academic Press, San Diego, 2000.

**Kinetic double layer
model (K2-SURF)**

M. Shiraiwa et al.

Title Page

Abstract	Introduction
Conclusions	References
Tables	Figures

◀ ▶

◀ ▶

Back Close

Full Screen / Esc

Printer-friendly Version

Interactive Discussion

Fuzzi, S., Andreae, M. O., Huebert, B. J., Kulmala, M., Bond, T. C., Boy, M., Doherty, S. J., Guenther, A., Kanakidou, M., Kawamura, K., Kerminen, V. M., Lohmann, U., Russell, L. M., and Pöschl, U.: Critical assessment of the current state of scientific knowledge, terminology, and research needs concerning the role of organic aerosols in the atmosphere, climate, and global change, Atmos. Chem. Phys., 6, 2017–2038, 2006, http://www.atmos-chem-phys.net/6/2017/2006/.

Gross, S. and Bertram, A. K.: Reactive uptake of NO_3, N_2O_5, NO_2, HNO_3, and O_3 on three types of polycyclic aromatic hydrocarbon surfaces, J. Phys. Chem. A, 112(14), 3104–3113, 2008.

Hallquist, M., Wenger, J. C., Baltensperger, U., Rudich, Y., Simpson, D., Claeys, M., Dommen, J., Donahue, N. M., George, C., Goldstein, A. H., Hamilton, J. F., Herrmann, H., Hoffmann, T., Iinuma, Y., Jang, M., Jenkin, M. E., Jimenez, J. L., Kiendler-Scharr, A., Maenhaut, W., McFiggans, G., Mentel, Th. F., Monod, A., Prévôt, A. S. H., Seinfeld, J. H., Surratt, J. D., Szmigielski, R., and Wildt, J.: The formation, properties and impact of secondary organic aerosol: current and emerging issues, Atmos. Chem. Phys., 9, 5155–5235, 2009, http://www.atmos-chem-phys.net/9/5155/2009/.

Hansen, J., Sato, M., and Ruedy, R.: Radiative forcing and climate response, J. Geophys. Res.-Atmos., 102(D6), 6831–6864, 1997.

Homann, K. H.: Fullerenes and soot formation – new pathways to large particles in flames, Angew. Chem. Int. Edit., 37(18), 2435–2451, 1998.

IUPAC (Ed.): Compendium of Chemical Terminology, 2nd ed. (the "Gold Book"), Blackwell Scientific Publications, Oxford, 1997.

Ivanov, A. V., Trakhtenberg, S., Bertram, A. K., Gershenzon, Y. M., and Molina, M. J.: OH, HO_2, and ozone gaseous diffusion coefficients, J. Phys. Chem. A, 111(9), 1632–1637, 2007.

Jacobson, M. Z.: A physically-based treatment of elemental carbon optics: Implications for global direct forcing of aerosols, Geophys. Res. Lett., 27(2), 217–220, 2000.

Kahan, T. F., Kwamena, N. O. A., and Donaldson, D. J.: Heterogeneous ozonation kinetics of polycyclic aromatic hydrocarbons on organic films, Atmos. Environ., 40(19), 3448–3459, 2006.

Kulmala, M., Asmi, A., Lappalainen, H. K., Carslaw, K. S., Pöschl, U., Baltensperger, U., Hov, Ø., Brenquier, J.-L., Pandis, S. N., Facchini, M. C., Hansson, H.-C., Wiedensohler, A., and O'Dowd, C. D.: Introduction: European Integrated Project on Aerosol Cloud Climate and Air Quality interactions (EUCAARI) – integrating aerosol research from nano to global scales,

Atmos. Chem. Phys., 9, 2825–2841, 2009,
http://www.atmos-chem-phys.net/9/2825/2009/.

Kuwata, M., Kondo, Y., Mochida, M., Takegawa, N., and Kawamura, K.: Dependence of CCN activity of less volatile particles on the amount of coating observed in Tokyo, J. Geophys. Res., 112, D11207, doi:10.1029/2006JD007758, 2007.

Kwamena, N. O. A., Earp, M. E., Young, C. J., and Abbatt, J. P. D.: Kinetic and product yield study of the heterogeneous gas-surface reaction of anthracene and ozone, J. Phys. Chem. A, 110(10), 3638–3646, 2006.

Kwamena, N. O. A., Staikova, M. G., Donaldson, D. J., George, I. J., and Abbatt, J. P. D.: Role of the aerosol substrate in the heterogeneous ozonation reactions of surface-bound PAHs, J. Phys. Chem. A, 111, 11050–11058, 2007.

Kwamena, N. O. A., Thornton, J. A., and Abbatt, J. P. D.: Kinetics of surface-bound benzo[a]pyrene and ozone on solid organic and salt aerosols, J. Phys. Chem. A, 108(52), 11626–11634, 2004.

Lammel, G., Sehili, A. M., Bond, T. C., Feichter, J., and Grassl, H.: Gas/particle partitioning and global distribution of polycyclic aromatic hydrocarbons – a modelling approach, Chemosphere, 76(1), 98–106, 2009.

Lee, J. Y. and Kim, Y. P.: Source apportionment of the particulate PAHs at Seoul, Korea: impact of long range transport to a megacity, Atmos. Chem. Phys., 7, 3587–3596, 2007, http://www.atmos-chem-phys.net/7/3587/2007/.

Liu, Y., Sklorz, M., Schnelle-Kreis, J., Orasche, J., Ferge, T., Kettrup, A., and Zimmermann, R.: Oxidant denuder sampling for analysis of polycyclic aromatic hydrocarbons and their oxygenated derivates in ambient aerosol: Evaluation of sampling artefact, Chemosphere, 62(11), 1889–1898, 2006.

Marchand, N., Besombes, J. L., Chevron, N., Masclet, P., Aymoz, G., and Jaffrezo, J. L.: Polycyclic aromatic hydrocarbons (PAHs) in the atmospheres of two French alpine valleys: sources and temporal patterns, Atmos. Chem. Phys., 4, 1167–1181, 2004, http://www.atmos-chem-phys.net/4/1167/2004/.

Masel, R. I.: Principles of Adsorption and Reaction on Solid Surfaces, John Wiley & Sons, New York, 1996.

Messerer, A., Rothe, D., Niessner, R., and Pöschl, U.: Kinetic observations and model calculations on continuous regeneration of NFZ diesel carbon particle precipitation systems, Chem.-Ing.-Tech., 77(7), 881–886, 2005.

[ACPD](#)

9, 18021–18063, 2009

Kinetic double layer model (K2-SURF)

M. Shiraiwa et al.

Title Page	
Abstract	Introduction
Conclusions	References
Tables	Figures

◄◄	►►
◄	►
Back	Close

Full Screen / Esc

Printer-friendly Version

Interactive Discussion

Mikhailov, E. F., Vlasenko, S. S., Podgorny, I. A., and Ramanathan, V.: Optical properties of soot-water drop agglomerates: An experimental study, J. Geophys. Res.-Atmos., 111(D7), 16, doi:10.1029/2005jd006389, 2006.

Mmereki, B. T. and Donaldson, D. J.: Direct observation of the kinetics of an atmospherically important reaction at the air-aqueous interface, J. Phys. Chem. A, 107(50), 11038–11042, 2003.

Mmereki, B. T., Donaldson, D. J., Gilman, J. B., Eliason, T. L., and Vaida, V.: Kinetics and products of the reaction of gas-phase ozone with anthracene adsorbed at the air-aqueous interface, Atmos. Environ., 38(36), 6091–6103, 2004.

Pitts, J. N.: Formation and fate of gaseous and particulate mutagens and carcinogens in real and simulated atmospheres, Environ. Health Persp., 47(Jan.), 115–140, 1983.

Pöschl, U.: Formation and decomposition of hazardous chemical components contained in atmospheric aerosol particles, J. Aerosol. Med., 15(2), 203–212, 2002.

Pöschl, U.: Atmospheric aerosols: Composition, transformation, climate and health effects, Angew. Chem. Int. Edit., 44(46), 7520–7540, 2005.

Pöschl, U., Letzel, T., Schauer, C., and Niessner, R.: Interaction of ozone and water vapor with spark discharge soot aerosol particles coated with benzo[a]pyrene: O_3 and H_2O adsorption, benzo[a]pyrene degradation, and atmospheric implications, J. Phys. Chem. A, 105(16), 4029–4041, 2001.

Pöschl, U., Rudich, Y., and Ammann, M.: Kinetic model framework for aerosol and cloud surface chemistry and gas-particle interactions – Part 1: General equations, parameters, and terminology, J. Phys. Chem. A, 7(23), 5989–6023, 2007.

Prinn, R., Cunnold, D., Simmonds, P., Alyea, F., Boldi, R., Crawford, A., Fraser, P., Gutzler, D., Hartley, D., Rosen, R., and Rasmussen, R.: Global average concentration and trend for hydroxyl radicals deduced from ALE/GAGE trichloroethane (methyl chloroform) data for 1978–1990, J. Geophys. Res.-Atmos., 97(D2), 2445–2461, 1992.

Rogaski, C. A., Golden, D. M., and Williams, L. R.: Reactive uptake and hydration experiments on amorphous carbon treated with NO_2, SO_2, O_3, HNO_3, and H_2SO_4, Geophys. Res. Lett., 24(4), 381–384, 1997.

Rudich, Y., Talukdar, R. K., Imamura, T., Fox, R. W., and Ravishankara, A. R.: Uptake of NO_3 on KI solutions: rate coefficient for the NO_3+I^- reaction and gas-phase diffusion coefficients for NO_3, Chem. Phys. Lett. 261(4–5), 467–473, 1996.

Sadezky, A., Muckenhuber, H., Grothe, H., Niessner, R., and Pöschl, U.: Raman microspec-

troscopy of soot and related carbonaceous materials: Spectral analysis and structural information, Carbon, 43(8), 1731–1742, 2005.

Schauer, C.: Analysis and reactivity of polycyclic aromatic hydrocarbon in aerosol, Technical University of Munich, 2004.

5   Schauer, C., Niessner, R., and Pöschl, U.: Polycyclic aromatic hydrocarbons in urban air particulate matter: Decadal and seasonal trends, chemical degradation, and sampling artifacts, Environ. Sci. Technol., 37(13), 2861–2868, 2003.

Schauer, C., Niessner, R., and Pöschl, U.: Analysis of nitrated polycyclic aromatic hydrocarbons by liquid chromatography with fluorescence and mass spectrometry detection: air particulate

10   matter, soot, and reaction product studies, Anal. Bioanal. Chem., 378(3), 725–736, 2004.

Schwarz, J. P., Gao, R. S., Spackman, J. R., Watts, L. A., Thomson, D. S., Fahey, D. W., Ryerson, T. B., Peischl, J., Holloway, J. S., Trainer, M., Frost, G. J., Baynard, T., Lack, D. A., de Gouw, J. A., Warneke, C., and Del Negro, L. A.: Measurement of the mixing state, mass, and optical size of individual black carbon particles in urban and biomass burning emissions,

15   Geophys. Res. Lett., 35(13), L13810, doi:10.1029/2008gl033968, 2008.

Segal-Rosenheimer, M. and Dubowski, Y.: Photolysis of thin films of cypermethrin using in situ FTIR monitoring: Products, rates and quantum yields, J. Photochem. Photobiol. A Chem., 200(2–3), 262–269, 2008.

Seinfeld, J. H. and Pandis, S. N.: Atmospheric Chemistry and Physics – From Air Pollution to

20   Climate Change, John Wiley & Sons, Inc., New York, 1998.

Shiraiwa, M., Kondo, Y., Moteki, N., Takegawa, N., Miyazaki, Y., and Blake, D. R.: Evolution of mixing state of black carbon in polluted air from Tokyo, Geophys. Res. Lett. 34(16), L16803, doi:10.1029/2007gl029819, 2007.

Springmann, M., Knopf, D. A., and Riemer, N.: Detailed heterogeneous chemistry in an ur-

25   ban plume box model: reversible co-adsorption of O_3, NO_2, and H_2O on soot coated with benzo[a]pyrene, Atmos. Chem. Phys. Discuss., 9, 10055–10099, 2009, http://www.atmos-chem-phys-discuss.net/9/10055/2009/.

Tabor, K., Gutzwiller, L., and Rossi, M. J.: Heterogeneous chemical-kinetics of NO_2 on amorphous-carbon at ambient temperature, J. Phys. Chem., 98(24), 6172–6186, 1994.

30   Wu, C. H., Salmeen, I., and Niki, H.: Fluorescence spectroscopic study of reactions between gaseous ozone and surface-adsorbed polycyclic aromatic-hydrocarbons, Environ. Sci. Technol., 18(8), 603–607, 1984.

Title Page

Abstract | Introduction

Conclusions | References

Tables | Figures

◄ | ►|

◄ | ►

Back | Close

Full Screen / Esc

Printer-friendly Version

Interactive Discussion

Table 1. Basic physicochemical parameters of O_3 in the PAH-O_3-H_2O system with different PAHs and substrates.

PAH	Substrate	RH(%)	K_{ads,O_3} $(10^{-15}\,cm^3)$	$k_{s,PAH,max}$ (s^{-1})	k_{SLR,PAH,O_3} $(10^{-17}\,cm^2\,s^{-1})$	k_{d,O_3} (s^{-1})	τ_{d,O_3} (s)	$\Delta H_{ads,O_3}$ $(kJ\,mol^{-1})$	Reference
BaP	Soot	25	255	0.0155	3.37	0.08	13.0	−86	Pöschl et al. (2001)
BaP	Azelaic acid	72	4.39	0.0600	10.4	3.56	0.28	−76	Kwamena et al. (2004)
BaP	Soot	0	255	0.0154	2.66	0.06	16.3	−86	Pöschl et al. (2001)
BaP	Azelaic acid	0	1.18	0.0480	8.30	13.2	0.08	−73	Kwamena et al. (2004)
BaP	NaCl	0	0.12	0.0320	5.54	130	0.01	−67	Kwamena et al. (2004)
BaP	Fused silica	0	27.1	0.0325	5.62	0.58	1.74	−81	Wu et al. (1984)
BaP	Silica gel	0	9.4	0.0325	5.62	1.67	0.60	−78	Alebic-Juretic et al. (1990)
Anthracene	Glass	0	2.85	0.0060	1.04	5.48	0.18	−75	Kwamena et al. (2006)
Anthracene	Azelaic acid	0	2.24	0.0550	9.52	6.97	0.14	−75	Kwamena et al. (2007)
BaA	Silica gel	0	38.6	0.004	0.69	0.40	2.47	−82	Alebic-Juretic et al. (1990)
Pyrene	Silica gel	0	86.0	0.001	0.17	0.18	5.51	−84	Alebic-Juretic et al. (1990)
Perylene	Silica gel	0	67.9	0.004	0.69	0.23	4.35	−83	Alebic-Juretic et al. (1990)
Perylene	Fused silica	0	4.4	0.004	0.69	3.55	0.28	−76	Wu et al. (1984)
Fluoranthene	Silica gel	0	65.0	0.0001	0.02	0.24	4.17	−83	Alebic-Juretic et al. (1990)
BaP	Octanol	0	0.35	0.0055	0.94	45.0	0.02	−70	Kahan et al. (2006)
Anthracene	Phenylsiloxane oil	0	104	0.0100	1.73	0.15	6.66	−84	Kwamena et al. (2007)
Anthracene	Octanol/decanol	0	0.56	0.0026	0.44	28.0	0.04	−71	Kahan et al. (2006)
Anthracene	Octanol	0	1.83	0.0026	0.45	8.53	0.12	−74	Mmereki et al. (2003)
Anthracene	Water	0	0.45	0.0026	0.45	34.7	0.03	−71	Mmereki et al. (2003)
Anthracene	Stearic aicd	0	0.47	0.0024	0.41	33.4	0.03	−71	Mmereki et al. (2004)
Anthracene	Octanoic acid	0	0.94	0.0013	0.22	16.7	0.06	−72	Mmereki et al. (2004)
Anthracene	Hexanoic acid	0	1.2	0.0004	0.07	13.0	0.08	−73	Mmereki et al. (2004)
Naphthalene	Octanol	0	0.97	0.0009	0.15	16.1	0.06	−72	Kahan et al. (2006)
Pyrene	Octanol	0	0.32	0.0007	0.12	48.8	0.02	−70	Kahan et al. (2006)
Pyrene	Water	0	0.86	0.0012	0.20	18.2	0.06	−72	Donaldson et al. (2005)
Pyrene	Octanol/water	0	1.66	0.0015	0.26	9.41	0.11	−74	Donaldson et al. (2005)
Phenanthrene	Octanol	0	0.16	0.0006	0.10	97.6	0.01	−68	Kahan et al. (2006)
SAM C3&C8	ZnSe	0	25	0.0060	1.04	0.62	1.60	−80	Dubowski et al. (2004)
Cypermethrin	ZnSe	0	0.47	0.0007	0.12	33.2	0.03	−71	Segal-Rosenheimer and Dubowski (2007)

Table 2. Basic physicochemical parameters of H_2O in the BaP-O_3-NO_2-H_2O system on soot and azelaic acid.

Substrate	RH (%)	K_{ads,H_2O} $(10^{-17}\,cm^3)$	$[SS]_{ss}$ $(10^{14}\,cm^{-2})$	τ_{d,H_2O} (s)	k_{d,H_2O} (s^{-1})	$\Delta H_{ads,H_2O}$ $(kJ\,mol^{-1})$		
Soot	25	0.17	4.60	1.33×10^{-4}	7.54×10^3	-35 ± 9	Pöschl et al. (2001)	$[O_3]_s$ vs. $[O_3]_{gs}$
Soot	25	0.15	2.24	5.69×10^{-5}	1.76×10^4	-33 ± 9	Schauer et al. (2003)	$[O_3]_s$ vs. $[O_3]_{gs}$
Soot	25	1.02	–	7.95×10^{-4}	1.26×10^3	-39 ± 9	Pöschl et al. (2001)	$k_{s,BaP}$ vs. $[O_3]_{gs}$
Soot	25	1.18	–	4.48×10^{-4}	2.23×10^3	-38 ± 9	Schauer et al. (2003)	$k_{s,BaP}$ vs. $[O_3]_{gs}$
Azelaic acid	72	0.10	–	9.80×10^{-5}	1.02×10^4	-34 ± 9	Kwamena et al. (2004)	$k_{s,BaP}$ vs. $[O_3]_{gs}$

Table 3. Basic physicochemical parameters of NO_2 in the BaP-O_3-NO_2-H_2O system on soot (Schauer, 2004).

RH (%)	NO_2 (ppb)	K_{ads,NO_2} (10^{-15} cm^3)	$[SS]_{ss}$ (10^{14} cm^{-2})	k_{d,NO_2} (s^{-1})	τ_{d,NO_2} (s)	$\Delta H_{ads,NO_2}$ (kJ mol^{-1})	
0	100	82	4.50	16.0	0.062	−70	$[O_3]_s$ vs. $[O_3]_{gs}$
0	500	34	3.50	49.6	0.020	−67	$[O_3]_s$ vs. $[O_3]_{gs}$
0	1000	53	3.00	37.1	0.027	−68	$[O_3]_s$ vs. $[O_3]_{gs}$
25	1000	10	2.24	263	0.004	−63	$[O_3]_s$ vs. $[O_3]_{gs}$
0	100	69	–	19.0	0.053	−69	$k_{s,BaP}$ vs. $[O_3]_{gs}$
0	250	54	–	27.3	0.037	−68	$k_{s,BaP}$ vs. $[O_3]_{gs}$
25	250	86	–	17.2	0.058	−70	$k_{s,BaP}$ vs. $[O_3]_{gs}$
0	500	71	–	23.8	0.042	−69	$k_{s,BaP}$ vs. $[O_3]_{gs}$
0	750	17	–	99.2	0.010	−65	$k_{s,BaP}$ vs. $[O_3]_{gs}$

Table 4. Basic physicochemical parameters of O_3 in the BaP-O_3-NO_2-H_2O system on soot (Schauer, 2004).

RH (%)	NO₂ (ppb)	K_{ads,O_3} (10^{-15} cm³)	$k_{s,PAH,max}$ (s⁻¹)	$[SS]_{ss}$ (10^{14} cm⁻²)	k_{SLR,PAH,O_3} (10^{-17} cm² s⁻¹)	k_{d,O_3} (s⁻¹)	τ_{d,O_3} (s)	$\Delta H_{ads,O_3}$ (kJ mol⁻¹)
0	0	255	0.015	5.80	2.66	0.06	16.3	−86
0	100	331	0.013	4.50	2.89	0.06	16.5	−86
0	250	369	0.015	**4.00**	3.75	0.06	16.4	−86
25	250	332	0.021	**4.00**	5.25	0.07	14.7	−86
0	500	347	0.020	3.50	5.71	0.07	13.5	−86
0	750	296	0.020	**3.25**	6.15	0.09	10.7	−85

The values in bold are interpolated values.

Table 5. Basic physicochemical parameters of O_3, H_2O, and NO_2 used in the numerical simulations of transient conditions.

	Substrate	K_{ads} $(10^{-15}\,cm^3)$	k_{SLR,PAH,O_3} $(10^{-17}\,cm^2\,s^{-1})$	τ_d (s)	$\alpha_{s,0}$	ω $(cm\,s^{-1})$
O_3	Soot	160	2.7	10	10^{-3}	3.60×10^4
	Organics	1.6–16	2.7	0.1–1	10^{-3}	3.60×10^4
	Liquid	0.16–1.6	0.5	0.01–0.1	10^{-3}	3.60×10^4
H_2O		10^{-3}	–	10^{-4}	4.0×10^{-4}	5.90×10^4
NO_2		50	–	0.05	0.064	3.69×10^4

Table 6. Chemical half-life of PAHs in the PAH-O_3-NO_2-H_2O system assuming different values for the O_3-NO_2 and PAH-NO_3 surface layer reaction rate coefficients (k_{SLR,O_3,NO_2}, k_{SLR,PAH,NO_3}).

$\tau_{d,NO_3}=10\,s$		k_{SLR,PAH,NO_3} (cm^2 s^{-1})			
	$t_{1/2}$ (s)	10^{-17}	10^{-16}	10^{-14}	10^{-11}
k_{SLR,O_3,NO_2}	10^{-18}	263	262	245	242
(cm^2 s^{-1})	10^{-17}	265	253	154	145
	10^{-16}	287	197	41	36
$\tau_{d,NO_3}=0.01\,s$		k_{SLR,PAH,NO_3} (cm^2 s^{-1})			
	$t_{1/2}$ (s)	10^{-17}	10^{-16}	10^{-14}	10^{-11}
k_{SLR,O_3,NO_2}	10^{-18}	263	263	263	244
(cm^2 s^{-1})	10^{-17}	266	266	264	153
	10^{-16}	297	297	280	40

Table A1. Frequently used symbols.

Symbol	Meaning
γ_{X_i}	Uptake coefficient of X_i
τ_{d,X_i}	Desorption lifetime of X_i
ω_{X_i}	Mean thermal velocity of X_i in the gas phase
C_{g,X_i}	Gas phase diffusion correction factor of X_i
d_p	Particle diameter
k_{d,X_i}	First-order desorption rate coefficient of X_i
k_{SLRv,X_p,X_q},	Second-order rate coefficients for surface layer reactions of X_p
k_{SLRv,X_p,Y_q}	with X_q, X_p with Y_q, respectively
K_{ads,X_i}	Adsorption equilibrium constant of X_i
K'_{ads,X_i}	Effective adsorption equilibrium constant of X_i
$\alpha_{s,0,X_i}$	Surface accommodation coefficient of X_i on an adsorbate-free surface
$t_{1/2}$	Chemical half-life of PAHs on the surface
$[SS]_{ss}$	Sorption site surface concentration
$[X_i]_g$	Gas phase concentration of X_i
$[X_i]_{gs}$	Near-surface gas phase concentration of X_i
$[X_i]_s$	Surface concentration of X_i (sorption layer)
$[Y_j]_{ss}$	Surface concentration of Y_j (quasi-static layer)
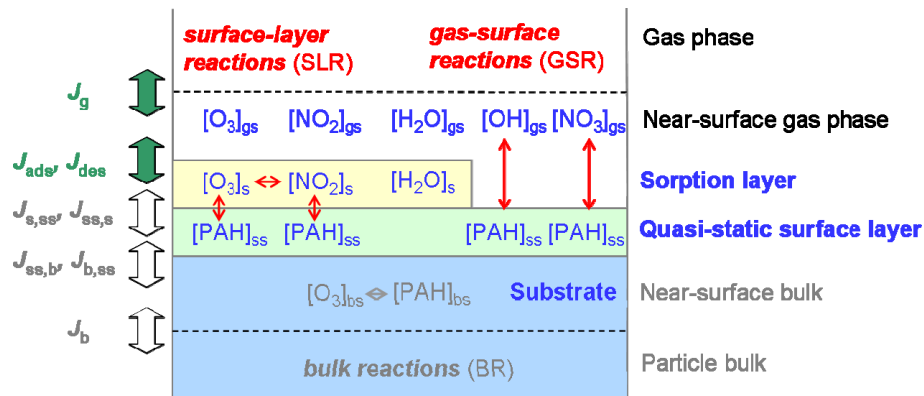
Fig. 1. Schematic illustration of the kinetic double-layer surface model (K2-SURF). Compartments and transport fluxes for volatile species (O_3, H_2O, NO_2, OH and NO_3) and non-volatile species (PAHs).
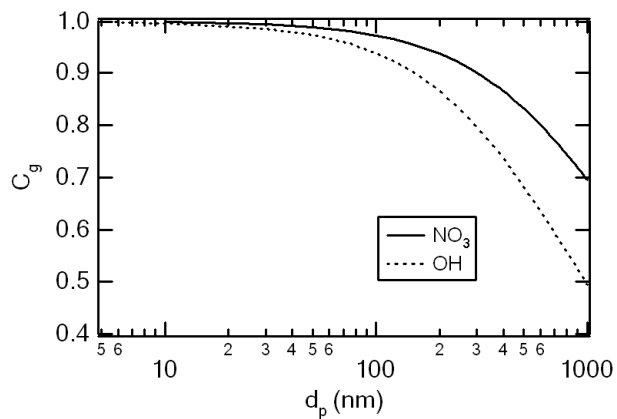
Fig. 2. Gas phase diffusion correction factor (C_g) for OH and NO_3 plotted against particle diameter (d_p).
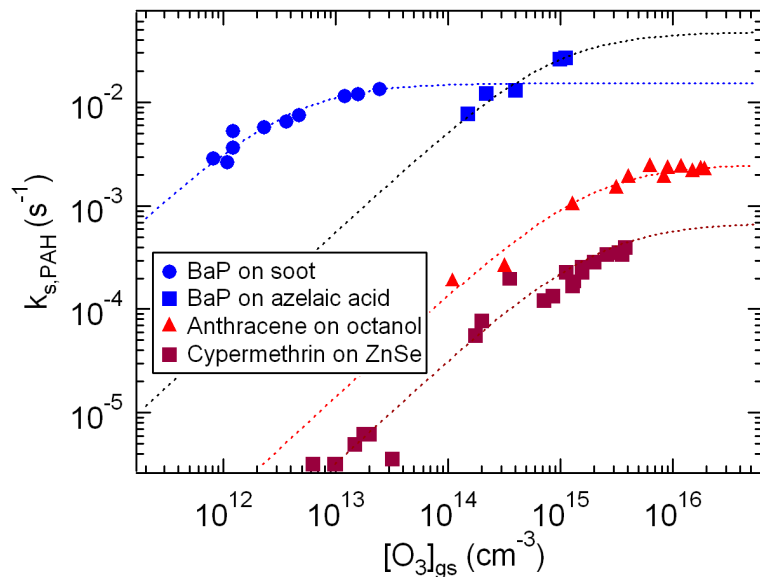
Fig. 3. Pseudo-first-order PAH decay rate coefficients ($k_{s,PAH}$) as a function of gas phase ozone concentration ($[O_3]_{gs}$) under dry conditions: BaP on soot aerosol (Pöschl et al., 2001), BaP on azelaic acid aerosol (Kwamena et al., 2004), Anthracene on octanol (Kahan et al., 2006), and cypermethrin on ZnSe (Segal-Rosenheimer and Dubowski, 2008).
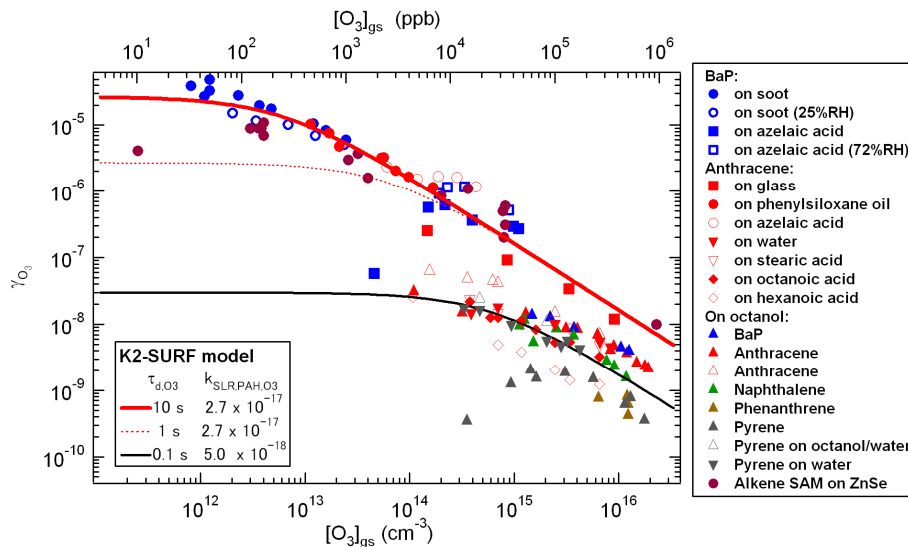
Fig. 4. Ozone uptake coefficients (γ_{O_3}) for different PAHs and substrates. Symbols represent literature data (Table 1). Lines show model results assuming the following parameters: 1) τ_{d,O_3}=10 s and k_{SLR,PAH,O_3}=2.7×10^{-17} for soot surfaces (red solid line), 2) τ_{d,O_3}=1 s and k_{SLR,PAH,O_3}=2.7×10^{-17} for solid organic surfaces (red dotted line), 3) τ_{d,O_3}=0.1 s and k_{SLR,PAH,O_3}=5.0×10^{-18} for liquid surfaces (black solid line).
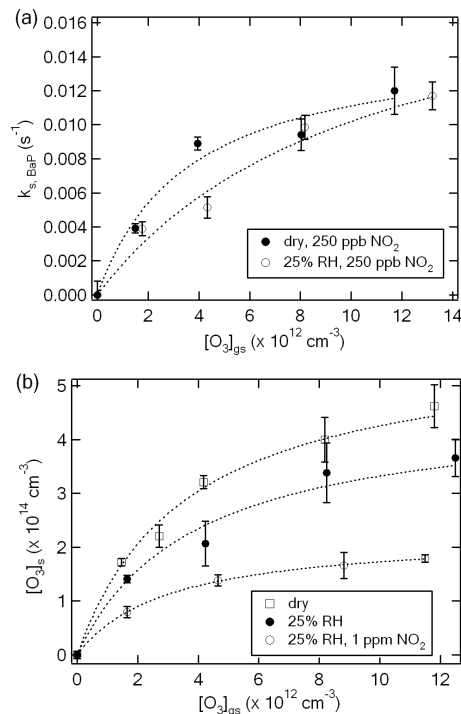
Fig. 5. Experimental data and fit lines for the BaP-O_3-NO_2-H_2O system (Schauer, 2004). **(a)** Pseudo-first-order BaP decay coefficients ($k_{s,BaP}$) as a function of gas phase ozone concentration ([O_3]$_{gs}$) under dry and wet (RH 25%) conditions with 250 ppb NO_2. **(b)** The surface concentration of ozone ([O_3]$_s$) as a function of [O_3]$_{gs}$. The data were measured under dry, wet (RH 25%), and wet (RH 25%) and NO_2 (1 ppm) conditions. Fit curves assume a Langmuir-Hishelwood-type mechanism.
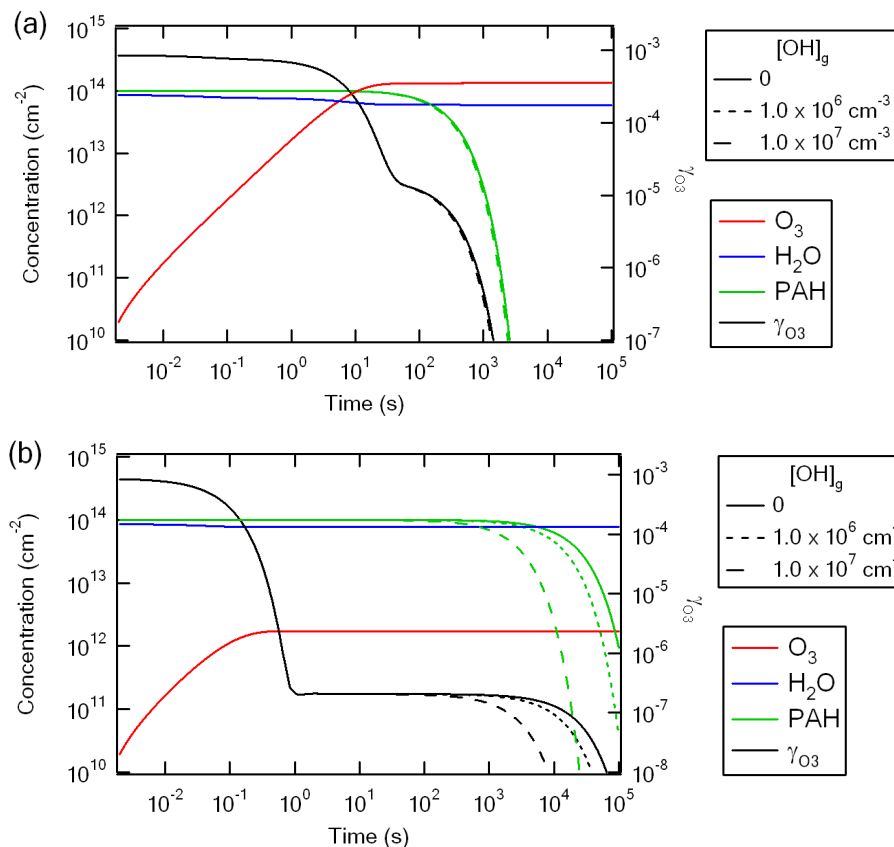
Fig. 6. Temporal evolution of the surface concentration of the volatile species (O_3 and H_2O), of PAH in the quasi-static surface layer, and of the ozone uptake coefficient (γ_{O_3}) at 100 ppb O_3 and 25% RH assuming OH concentration of 0 (solid line), 1.0×10^6 cm^{-3} (dotted line) and 1.0×10^6 cm^{-3} (dashed line). PAHs are either **(a)** on soot or **(b)** on a solid organic surface.
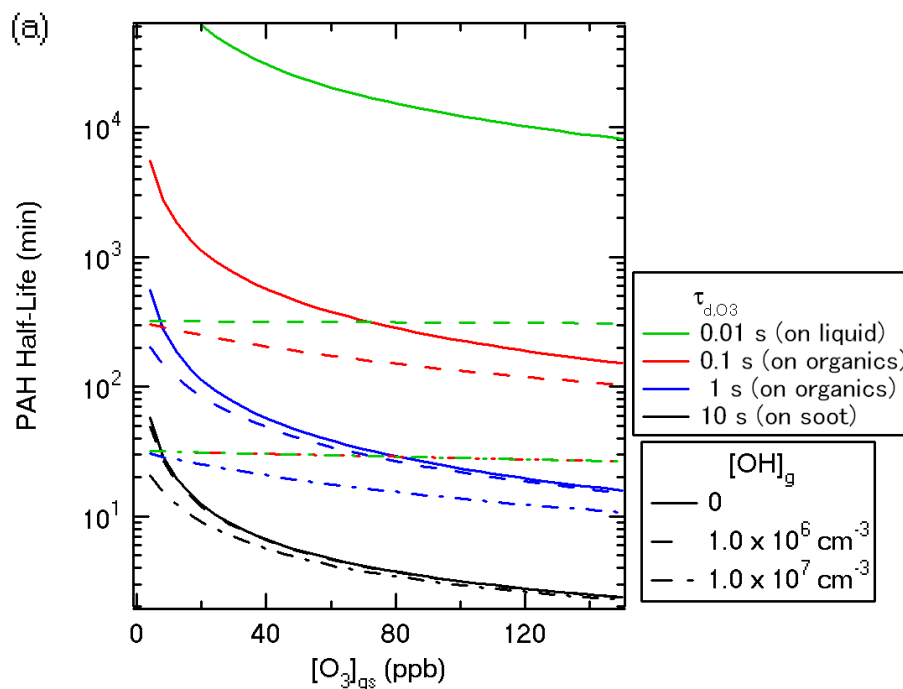
Fig. 7. Chemical half-life of PAHs on different substrates (soot, solid organic, liquid) as a function of gas phase ozone concentration at 25% RH assuming OH concentrations of 0 (solid lines), 1.0×10^6 cm^{-3} (dashed lines), and 1.0×10^7 cm^{-3} (dotted lines). The desorption lifetime of O_3 (τ_{d,O_3}) was set to 10 s (soot), 1 or 0.1 s (solid organic), and 0.01 s (liquid), respectively.
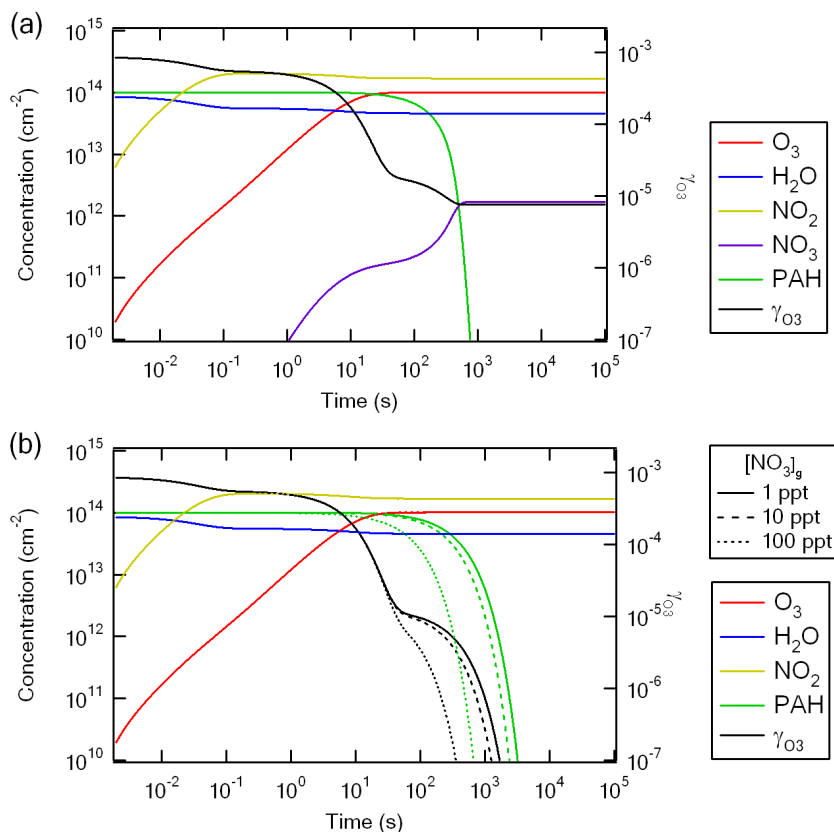
Fig. 8. Temporal evolution of the surface concentrations of PAHs and volatile species (O_3 and H_2O) on soot, and of the ozone uptake coefficient (γ_{O_3}) at 100 ppb O_3, 500 ppb NO_2 and 25% RH. **(a)** PAH-O_3-H_2O-NO_2 system considering surface reaction of O_3 with NO_2. **(b)** PAH-O_3-H_2O-NO_2-NO_3 system assuming NO_3 concentrations of 1 ppt (solid line), 10 ppt (dashed line) and 100 ppt (dotted line), respectively.
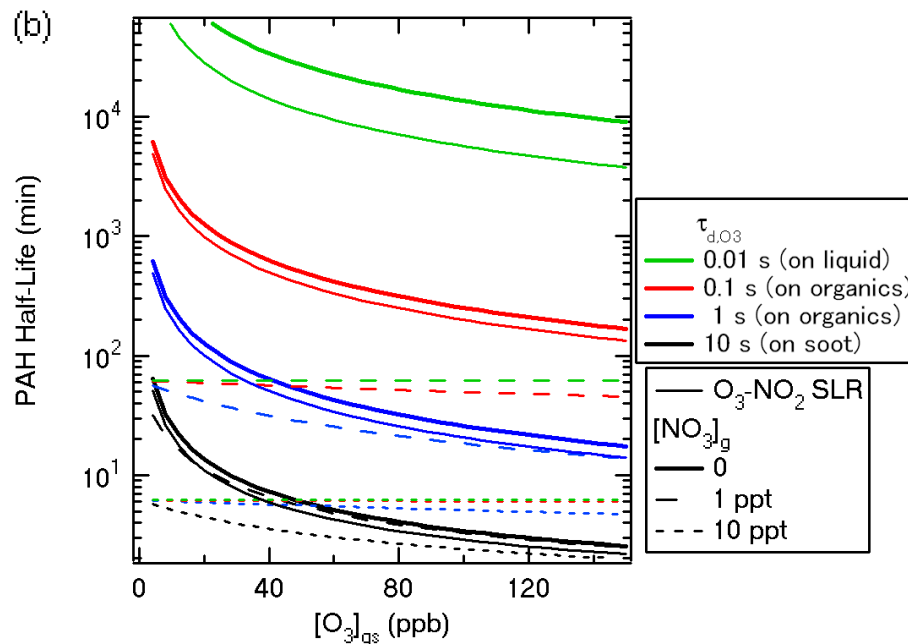
Fig. 9. Chemical half-life of PAHs on different substrates (soot, solid organic, liquid) as a function of gas phase ozone concentration at 100 ppb NO_2 and 25% RH. The desorption lifetime of O_3 (τ_{d,O_3}) is set to 10 s (soot), 1 or 0.1 s (solid organic), and 0.01 s (liquid), respectively. The assumed NO_3 gas phase concentrations are 0 (thick solid lines), 1 ppt (dashed lines), and 10 ppt (dotted lines), respectively. Thin solid lines indicate that O_3-NO_2 surface layer reactions are taken into account assuming $[NO_3]_g$=0.